ACS OMEGA

http://pubs.acs.org/journal/acsodf

Article

High-Porosity Polymer Composite for Removing Oil Spills in Cold Regions

Pham Le Quoc,* Alexandra Y. Solovieva, Mayya V. Uspenskaya, Roman O. Olekhnovich, Vera E. Sitnikova, Inna E. Strelnikova, and Anisa M. Kunakova

Cite This: *ACS Omega* 2021, 6, 20512–20521

Read Online

ACCESS | Metrics & More | Article Recommendations | Supporting Information

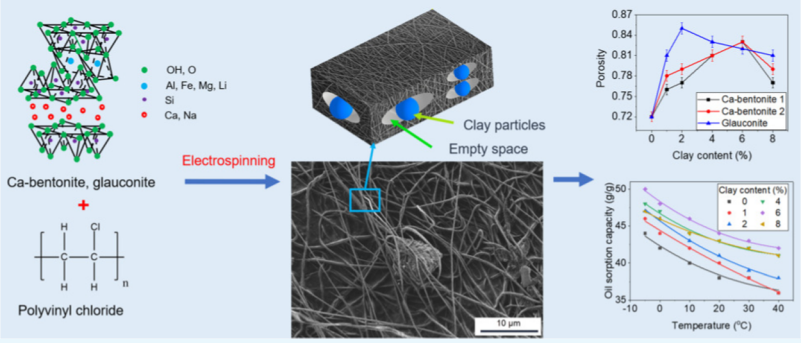

ABSTRACT: In this work, polyvinyl chloride (PVC)/clay nanofiber composites with various contents were fabricated by the electrospinning process. The morphology, porosity, density, and mechanical properties of the nanofiber mats were investigated. In addition, PVC/clay nanofiber mats were characterized by Fourier transform infrared spectroscopy, differential scanning calorimetry, and thermogravimetric analysis. Moreover, the influence of the clay content in the nanofiber mats and its effect on oil sorption capacity were also evaluated. The results show that the clay particle diameter affects the fabrication, morphology, porosity, density, mechanical properties, and sorption capacity of the nanofiber mats. Adding clay in nanofiber composite materials leads to higher porosity and a higher oil sorption capacity. PVC/clay nanofiber mats have a high oil sorption capacity at low temperatures. They exhibit a high potential to be used as materials to eliminate oil spills under arctic conditions.

INTRODUCTION

Currently, along with many environmental problems that need to be overcome and treated, such as greenhouse effects, air pollution, and water pollution, the oil spill treatment problem is an urgent issue. An oil spill occurs due to exploiting, transporting, and storing oil for industrial use and human activities. The oil spill affects the seawater quality and marine ecosystems, such as flora and fauna, same as communities around the affected area.[1] When an oil spill occurs, it is necessary to collect and handle it quickly to minimize its harmful effects on the environment. Many methods of dealing with oil spills, such as the mechanical method, microorganisms, chemical dispersion, and sorbent, are used, among which, the sorbent is a highly effective method and of low cost than other methods.[2] Recently, one type of potential material used to absorb oil that has caught the attention of scientists is the nanofiber sorbent.[3,4]

In recent decades, along with the development of nanomaterials, nanofiber polymers have also attracted the attention of many scientists. Polymer nanofibers have many outstanding properties compared to previously known fibers, such as a small diameter, large surface area, high porosity, and high mechanical strength, among others. They are found in various fields such as water filtration, air purification, water, oil separation, drug delivery, tissue engineering, energy storage, reinforcement components in composites, and other fields.[5] There are various methods for nanofiber polymer synthesis, such as drawing, template synthesis, self-assembly, melt-blowing, phase separation, and electrospinning.[6] Electrospinning is an effective method to fabricate nanofibers, thanks to its advantages such as a simple method, high efficiency, continuous process, adjustable size, and nanofiber orientation.[7] In addition, in recent years, many companies have started to produce equipment to manufacture nanofibers on a larger scale, thereby increasing the potential application of nanofibers in many different fields.[8]

One of the advantages of the electrospinning method is that it can fabricate a nanofiber composite polymer from a mixture of

Received: May 13, 2021
Accepted: July 16, 2021
Published: July 27, 2021

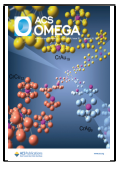

polymer−polymer or a mixture of polymers with different particles. Nanofibers demonstrate to have many superior properties in the presence of particles compared to nanofibers from the pure polymer. Nowadays, the fabrication of materials by combining polymers with clays has captured the interest of researchers due to the many outstanding properties suitable for application in different fields. One method of combining polymers and clay particles is using the electrospinning process to fabricate polymer/clay nanofibers. Clays tend to combine with molecules of the polymer chain, thereby increasing the mechanical strength of the nanofiber mats. Many studies report that adding clays to polymers leads to an increase in their mechanical strength, improved thermal properties, increased fire resistance, and heavy metal adsorption capacity of the nanofiber mat.[9,10] Shami and Sharifi-Sanjani[11] reported that the addition of Na-montmorillonite resulted in a decrease in diameter and improved thermal properties of polyacrylonitrile (PAN) nanofibers. Hong et al.[12] have fabricated composite nanofibers based on polyurethane (PU) and organically modified montmorillonite. Research results show that the presence of clay leads to an improved tensile strength and Young's modulus of PU/clay nanofiber mats.

Various clay types exist in nature, such as kaolinite, montmorillonite, vermiculite, and chlorite.[13] Each type has different characteristics and properties, such as the ability to absorb and swell. Some of the clays capable of absorbing heavy metals such as Fe, Cu, Pb, Cr, and oil are bentonite clay and glauconite clay. Bentonite clays have high water absorption and swelling capacity. There are two main types of bentonites in the industry: sodium and calcium bentonite. Structurally, bentonite includes around 60−70% montmorillonite, with a molecular formula $Si_8Al_4O_{20}(OH)_4$ in which Si has to be replaced by various metal cations such as sodium, calcium, zinc, iron, and others.[14] Nanofibers have been successfully fabricated from the mixture of montmorillonite with polymers such as nylon-6,[15] PAN,[16] poly(vinyl alcohol),[17] polylactic acid,[18] PU,[12] and cellulose acetate[19] for different purposes. For example, Silva et al.[20] have fabricated polyvinyl alcohol polyaniline-montmorillonite clay nanofibers for heavy metal filtration and as gas sensors.

Polyvinyl chloride (PVC), nowadays, is the cheapest and most commercially available polymer on the market. PVC is an amorphous polymer with high mechanical and chemical resistance under different environments such as acids and bases. Thanks to these superior properties, PVC finds many applications in various industries such as construction, packaging, oil pipeline making, and medical equipment.[21] PVC nanofibers have been successfully fabricated and have the potential for their implementation in many areas such as air filtration,[22] water treatment,[23] oil−water separation,[24] anticorrosion materials,[25] and materials for terahertz optical components.[26] However, the research on PVC/clay nanofiber fabrication is still lacking. Adding clay in PVC solution in order to fabricate nanofiber mats promises to increase its mechanical strength and oil sorption capacity, from which we can obtain materials with good oil sorption capacity and can be applied for oil−water separation.

In this study, we present the fabrication process of electrospun PVC/clay nanofibers. We have investigated the morphology, porosity, mechanical strength, and thermal properties of electrospun PVC/clay nanofibers. At the same time, we have studied the sorption capacity of PVC/clay nanofibers for different oils at different temperatures. PVC/clay nanofiber mats can be used for oil−water separation and are contributing to oil spill removal.

RESULTS AND DISCUSSION

Diameter of the Clay Particles. Figure 1 shows the particle diameter distribution of clay particles. Analysis results showed

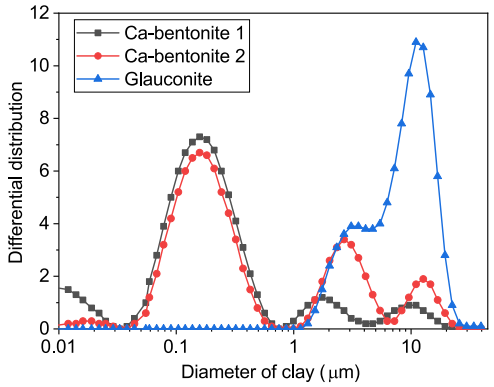

Figure 1. Differential distribution of the clay particle diameter.

that glauconite particles have the largest diameter and Ca-bentonite 1 particles have the smallest diameter. The average diameter of Ca-bentonite 1 particles is approximately 0.1 μm. The diameter distribution graph of Ca-bentonite 2 shows the particles distributed at two peaks which are 0.1 and 2 μm. The average particle diameter of glauconite is approximately 10 μm. Nonuniform distribution of the clay particles is possible due to aggregation of the particles in distilled water.

Characteristics of Electrospun PVC/Clay Nanofibers. *Morphology of Electrospun PVC/Clay Nanofibers.* The morphology of PVC/clay nanofibers is shown in Figure 2. The

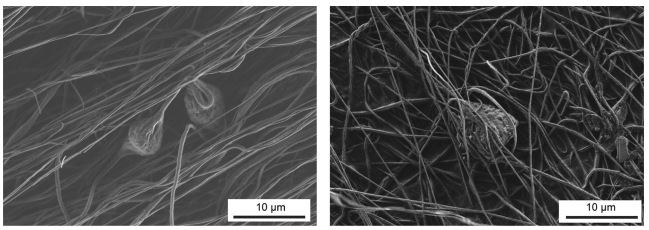

Figure 2. SEM images of electrospun PVC/clay nanofibers: (a)—2% Ca-bentonite 2 and (b)—6% Ca-bentonite 2.

scanning electron microscopy (SEM) image of PVC/clay shows that the nanofiber mat contains clay particles. Clay particles are distributed in the empty space of the mat or covered with PVC. Small clay particles will be covered with PVC, while larger clay particles will reside in the empty spaces of the nanofiber mat.

Figure 3a and Table 1 show the dependence of the nanofiber diameter on clay content. From the graph, it can be seen that when the clay content increases, it decreases the diameter of the nanofibers. Adding clay particles to the solution may led to an increase in the conductivity because the clay contains cations (Figure 3b). Thus, during the electrospinning process, the solution is subjected to a more significant electric field force, and smaller nanofibers are fabricated. We assume that Ca-bentonite is smaller in size than glauconite so that they are better at dissolving cations in solution. Therefore, solutions containing Ca-bentonite are affected by electric field force more strongly

https://doi.org/10.1021/acsomega.1c02517
ACS Omega 2021, 6, 20512−20521

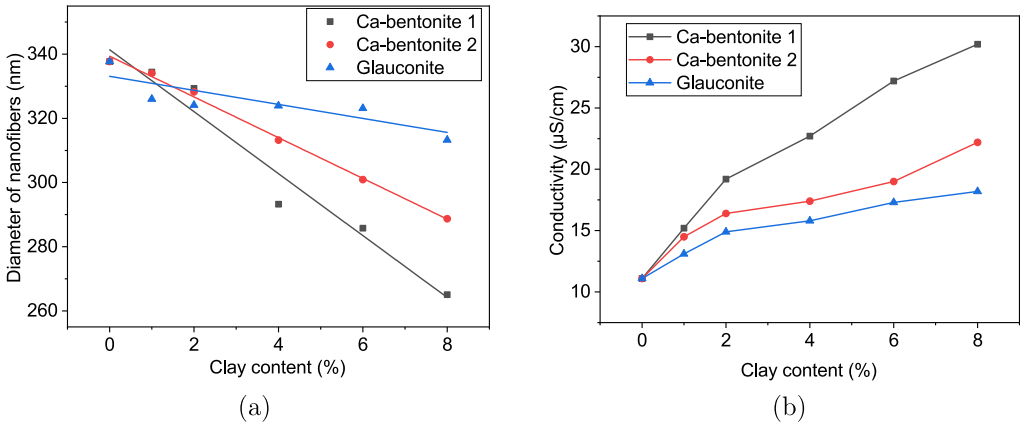

Figure 3. Dependence of the nanofiber diameter (a) and conductivity (b) on clay content.

Table 1. Diameter and Standard Deviations of PVC/Clay Nanofibers

	PVC/Ca-bentonite 1 nanofibers		PVC/Ca-bentonite 2 nanofibers		PVC/glauconite nanofibers	
clay content (%)	diameter (nm)	standard deviations (nm)	diameter (nm)	standard deviations (nm)	diameter (nm)	standard deviations (nm)
0	338	38	338	38	338	38
1	334	37	334	28	326	37
2	329	41	328	38	324	40
4	293	41	313	30	324	41
6	286	37	301	30	323	43
8	265	38	289	28	313	42

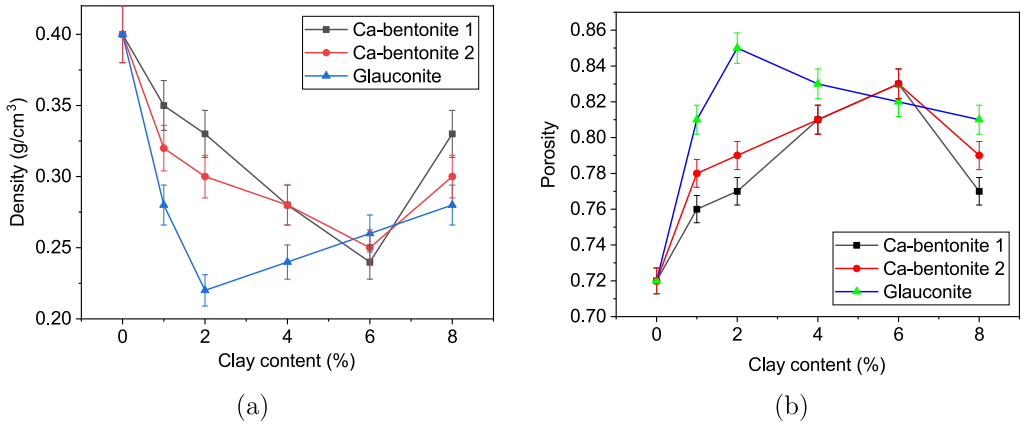

Figure 4. Density and porosity of PVC/clay nanofiber mats with different clay contents: (a)—density and (b)—porosity.

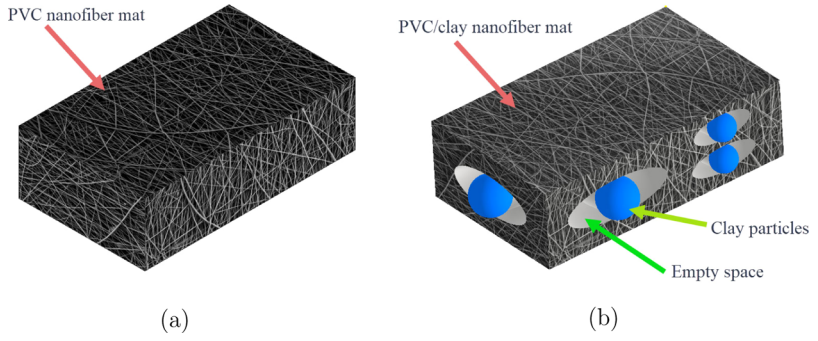

Figure 5. Representation of the nanofiber mat structure: (a)—PVC nanofiber mat and (b)—PVC/clay nanofiber mat.

than a solution containing glauconite. Therefore, the diameter of PVC/Ca-bentonite nanofibers is smaller than that of PVC/glauconite nanofibers. This phenomenon was also found in the study of PAN/Na-montmorillonite nanofibers[11] and PU/clay nanofibers.[12]

Figure 4 shows the density and porosity of the PVC/clay nanofiber mats. The density of PVC/clay nanofiber mats is

https://doi.org/10.1021/acsomega.1c02517
ACS Omega 2021, 6, 20512−20521

lower than that of pure PVC nanofiber mats. As mentioned above, the clay particles in the nanofiber mat can appear in two forms, either covered with polymer or alternating between nanofibers. In case the clay particles are located in the void space of the mat, it will create a lifting effect of the nanofibers in the mat, so there will be more empty space in the nanofiber mat. In summary, the presence of clay particles led to an increase in the void space of the nanofiber mat, which changed the mass of the nanofiber mat. Therefore, the density of PVC/clay nanofiber mats containing clays is lower than that of pure PVC nanofiber mats. For PVC/glauconite nanofiber mats, the lowest density was found when the glauconite content reaches 2%, while for PVC/bentonite nanofiber mats, the lowest density was found when bentonite content reaches 6%. This is due to the influence of the particle diameter of the clay during the electrospinning process. The change in density leads to a change in the porosity of the nanofiber mat. The porosity of the nanofiber mats containing glauconite was the highest, and that of the nanofiber mats containing Ca-bentonite 1 was the lowest due to the smallest diameter of Ca-bentonite 1 particles. Figure 5 illustrates the PVC/clay nanofiber mat with the empty spaces (voids) formed by clay particles and PVC nanofibers.

The density of the clay is higher than that of PVC. Therefore, under normal circumstances, mixing clay and PVC will increase the density of the mixture. However, the change in mass of the nanofiber mat is influenced by two factors. First, the mass reduction is caused by the formation of voids between the clay and the nanofiber mat. The second is the increase in mass caused by increasing the clay content. Hence, the density of the nanofiber mat decreases when the first factor is higher than the second factor. Conversely, the density of the nanofiber mat increases when the first factor is smaller than the second factor. Therefore, the increase in density and the decrease in porosity occur after the minima and maxima.

Contact Angle of PVC/Clay Nanofiber Mats. Figure 6 shows the contact angle measurement results of PVC/clay nanofiber mats. It can be seen that PVC/clay nanofiber mats are hydrophobic materials. There was no linear change in contact angle for different clay contents. The contact angle of PVC/clay nanofiber mats does not present significant changes, possibly because the clay is covered with the polymer or is in the space of the mat. In addition, the surface of the nanofiber mat is uneven; hence, there are significant deviations when measuring different positions of the sample, which may be the cause of the irregular distribution of the contact angle.

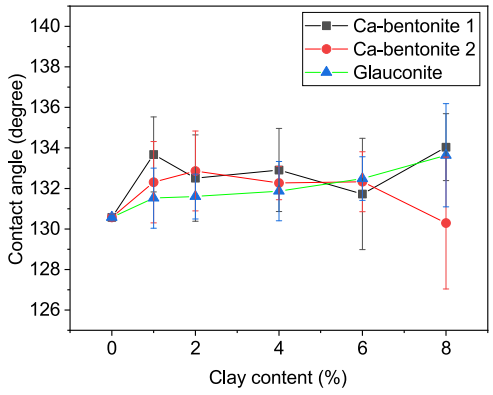

Figure 6. Contact angle of PVC/clay nanofiber mats.

Mechanical Properties of PVC/Clay Nanofiber Mats. Figure 7 shows the influence of clay content on the mechanical properties of PVC/clay nanofiber mats. It can be seen that varying clay contents leads to a change in tensile strength and Young's modulus of the nanofiber mats. For PVC/Ca-bentonite 1 and PVC/Ca-bentonite 2 nanofiber mats, the tensile strength and Young's modulus increased when the clay content increases from 0 to 4% and decreased when the clay content increases from 4 to 8%. For PVC/glauconite nanofiber mats, the tensile strength and Young's modulus increased when clay content increases from 0 to 1% and decreased when clay content increases from 1 to 8%. These results show that clay particles are effective to enhance the mechanical strength of nanofiber mats. Similar results were observed for electrospun pullulan/montmorillonite nanofiber mats.[27] In this work, clay particles have a main component of montmorillonite, consisting of two tetrahedral layers and one octahedral layer enclosed between them.[28] When the polymer and clay are dissolved in the solvent, the polymer can flow into space between the layers of the clay. Therefore, the bonding of the polymer and clay particles is improved, leading to an increase in the mechanical strength of the nanofiber mats. In addition, the enhancement of the mechanical strength is explained by the effect of molecular chain orientation.[29] The mechanical strength enhancement of the nanofiber mats may be caused by a decrease in the nanofiber diameter.[30] However, in the solvent, the clay particle tends to combine, to form large-sized clay blocks. Hence, when the clay content is high, the electrospinning process fabricated nanofiber mats with many defects. This phenomenon explains why the mechanical strength of PVC/clay nanofiber mats is reduced when the Ca-bentonite content is higher than 4% and glauconite is higher than 1%.

It can be seen that the increase in mechanical strength is caused mainly by the small diameter of clay particles linked to the polymer during the process of nanofiber fabrication, while the large diameter of clay particles plays the role of enhancement porosity. Because the particle diameter of Ca-bentonite is significantly smaller than that of glauconite, the Ca-bentonite content that can be blend into polymers will be higher than glauconite content. Therefore, the highest mechanical strength of PVC/Ca-bentonite is achieved when Ca-bentonite content is 4% and that of PVC/glauconite is reached when glauconite content is 1%.

FTIR Analysis. Fourier transform infrared (FTIR) spectra present structural information of the clays and PVC nanofiber mats. Figure 8 shows the spectra in the 400−4000 cm^{-1} range of PVC nanofibers, Ca-bentonite 1, and PVC/Ca-bentonite 1 nanofibers (see Supporting Information for more details on the thermal properties of PVC/Ca-bentonite 2 and PVC/glauconite nanofiber mats). In particular, FTIR spectra of clay particles in general and Ca-bentonite 1 particles are shown at two peaks representing O−H and Si−O functional groups at 3620 and 993 cm^{-1}, respectively.[31] The FTIR spectrum for PVC nanofibers showed the characteristic absorption bands of 613 cm^{-1}, which correspond to C−Cl stretching. The absorption band at 2908 cm^{-1} is assigned to C−H stretching, 1427 cm^{-1} is assigned to CH_2 deformation, 1253 cm^{-1} is assigned to CH-rocking, and 964 cm^{-1} is assigned to trans CH wagging.[32] The spectrum of PVC/clay nanofiber samples was observed to be similar to pure PVC nanofibers and did not show any characteristic peaks of clays. Two reasons that can explain this result are as follows: first, the clay content in PVC nanofiber mats is very small (from 1 to 8%) and second, clay particles are covered with polymers or

https://doi.org/10.1021/acsomega.1c02517
ACS Omega 2021, 6, 20512−20521

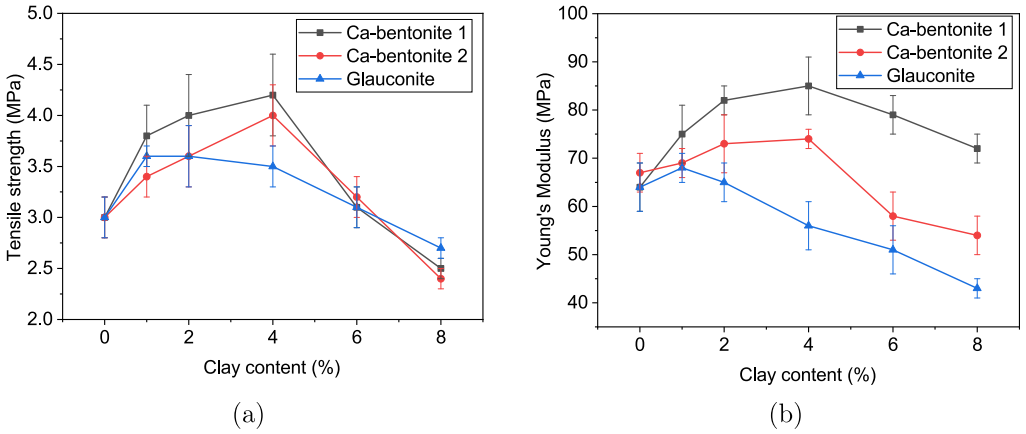

Figure 7. Effect of clay content on the mechanical properties of PVC/clay nanofiber mats: (a)—tensile strength and (b)—Young's modulus.

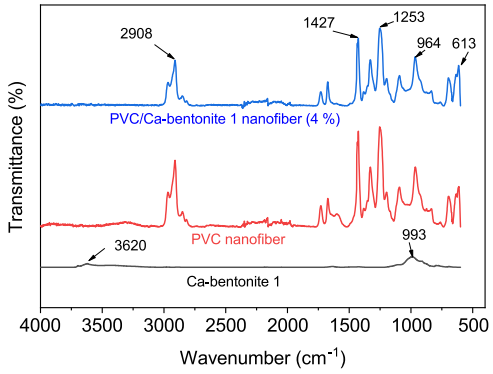

Figure 8. FTIR data spectra of PVC nanofibers, Ca-bentonite 1, and PVC/Ca-bentonite 1 nanofibers (4%).

located in empty space of the nanofiber mats. Similar results were found for the PVC/Na-sebacate organoclay nanocomposite.[33]

The spectrum of PVC nanofiber mats after oil removal shows that no new chemical bonds are formed (Figure 9). It shows that

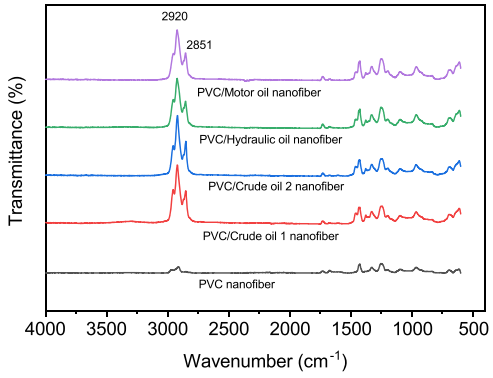

Figure 9. FTIR spectrum of PVC nanofiber mats after removal of oil.

the oil does not change the structure of PVC nanofibers. The spectrum of PVC nanofibers after oil removal also shows that the peaks at 2920 and 2851 cm^{-1} represent the C−H bonding of the oil.

Thermal Stability of PVC/Clay Nanofibers. Figure 10 shows the thermogravimetric analysis (TGA) and differential thermal analysis (DTA) of PVC and PVC/Ca-bentonite 1 nanofiber mats. The TGA and DTA thermogram shows that the degradation process of PVC nanofiber mats occurs in two stages.[30] There was no significant change in TGA of PVC/clay nanofiber mats compared to PVC nanofiber mats. Table 2 presents the TGA results of all samples, including the temperature of onset decomposition, the temperatures of the finish decomposition, and mass loss. The first stage of decomposition begins at 226 °C and finishes at 376 °C, with a mass loss of 58.7%. The second stage of decomposition begins at 376 °C and finishes at 532 °C, with a total mass loss of 86.4%. Table 2 also presents the DSC analysis results of PVC and PVC/Ca-bentonite 1 nanofiber mats. Results showed that there was no difference in glass transition temperature for nanofiber polymers when clay was added.

XRD Data of PVC/Clay Nanofibers. X-ray diffraction (XRD) patterns of PVC/clay nanofiber mats are shown in Figure 11. PVC is an amorphous polymer shown by a broad peak from 15 to 30° (2θ) on the diffraction plot.[34,35] Peaks at 29.5, 36, 39.5, 43, 47, and 48.5° (2θ) represent components of the PVC compound (including the thermal stabilizer and lubricants). For clays with the main composition of montmorillonite, the diffraction plot will show a characteristic peak in the range from 3 to 9° (2θ). In Figure 11, no peak is observed between 3 and 9° (2θ). This can be explained because clay particles can be located in the voids of nanofiber mats or be covered by the polymer, as mentioned above. Similar results are also observed for the composite of the hydrophobic polymer PU with clay.[36] In addition, there is no change in the intensity and width of the peaks; hence, the addition of clay does not change the degree of crystallinity and amorphousness of the nanofiber mats.

Study of Oil Sorption Capacity of PVC/Clay Nanofibers. *Effect of Clay Content on Sorption Capacity.* Figure 12 shows the sorption capacity of PVC/clay nanofiber mats for motor oil and water (see Supporting Information for details on sorption capacity for other oils). The presence of clay particles into nanofiber mats leads to an increase in their sorption capacity. For PVC/Ca-bentonite 1 and PVC/Ca-bentonite 2 nanofiber mats, sorption capacity increased when the clay content increased from 0 to 6%; on the other hand; it decreased when the clay content increased from 6 to 8%. The sorption capacity of PVC/glauconite nanofiber mats increases when the content of glauconite increased from 0 to 2% and decreased when the content of glauconite increased from 2 to 8%. The increase in the sorption capacity of nanofiber mats resulted due to an increase in the porosity of the nanofiber mats. It can be seen that the water adsorption capacity of PVC/clay nanofiber mats is higher than that of PVC nanofiber mats. Clay particles

https://doi.org/10.1021/acsomega.1c02517
ACS Omega 2021, 6, 20512−20521

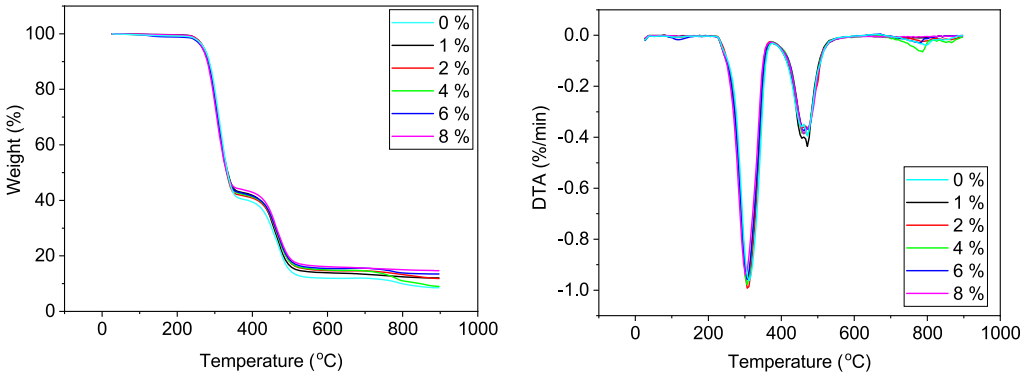

Figure 10. TGA and DTA thermogram of PVC and PVC/Ca-bentonite 1 nanofiber mats.

Table 2. TGA and DSC Data of PVC and PVC/Ca-Bentonite 1 Nanofiber Mats

	TGA							DSC	
	1st stage			2nd stage					
sample	T_{onset}, °C	T_{fd}, °C	mass loss, %	T_{onset}, °C	T_{fd}, °C	mass loss, %	residue after 800 °C, %	glass transition temperature, T_g, °C	melting temperature, T_m, °C
Ca-bentonite 1	253	322	2.1						192.1
Ca-bentonite 2	461	477	0.4						179.5
glauconite									159.9
PVC	226	376	58.7	376	532	86.4	89.1	77.7	
PVC/Ca-bentonite 1 (1%)	226	372	56.7	372	533	85	87.1	80.0	
PVC/Ca-bentonite 1 (2%)	226	370	57.5	370	533	83.9	86.1	81.2	
PVC/Ca-bentonite 1 (4%)	226	372	56.9	372	532	83.3	88.2	80.9	
PVC/Ca-bentonite 1 (6%)	226	370	56.1	370	533	82.5	84.9	77.7	
PVC/Ca-bentonite 1 (8%)	226	370	55.5	370	533	82.5	84.4	80.5	

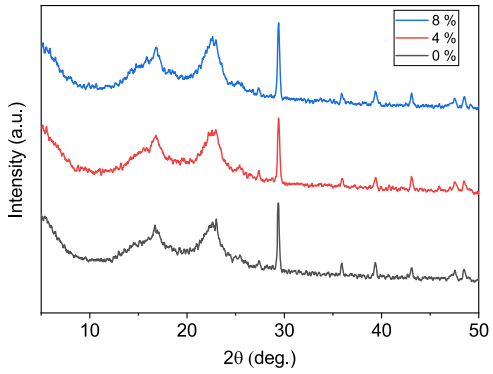

Figure 11. XRD patterns of PVC/clay nanofiber mats.

have a high affinity for water; hence, adding them to the nanofiber mats led to enhance the water sorption capacity of the nanofiber mats.

In general, sorbent materials can work under two mechanisms: absorption or adsorption. The adsorption mechanism is a process that occurs when a liquid is absorbed on the surface and leads to swelling of the material. Materials that work according to this mechanism are suitable for the removal of oils with low viscosity. The absorption mechanism is the process in which a liquid has flowed into the empty space of the material, and in this case, the liquid can be separated easily from the material under the action of the compression process.[37] Two factors can explain the oil sorption mechanism of the nanofiber mats: first, the oil flows into the empty space of the nanofiber mats and second, due to the bonding between the oil molecule and the surface of the nanofiber under the action of van der Waals force.[24,38]

The excellent sorption capacity of PVC/clay nanofiber mats can be explained by the following reasons. PVC has a surface tension of about 32−38 mN/m.[39] This value is higher than the surface tension of the oils (20 mN/m) and lower than the surface tension of seawater (60−65 mN/m). Therefore, the PVC-based materials have great potential for oil sorption and oil−water separation applications.[37] Moreover, PVC nanofiber mats have higher porosity; hence, they can hold a larger concentration of oil in the empty space of the mats. In addition, PVC nanofibers have a high surface area, thereby enhancing the oil sorption capacity.

Influence of Temperature on Oil Sorption Capacity. Temperature is one of the factors that strongly affect the oil sorption capacity of the nanofiber mat. The ambient temperature varies depending on the season and the region, especially in low-temperature regions such as the arctic. Therefore, it is essential to evaluate the oil absorption at different temperatures to determine the suitability of the implementation of the nanofiber mats. Figure 13 shows the effect of temperature on the sorption capacity of PVC/Ca-bentonite 1 nanofiber mats for different oils (see Supporting Information for details about the

https://doi.org/10.1021/acsomega.1c02517
ACS Omega 2021, 6, 20512−20521

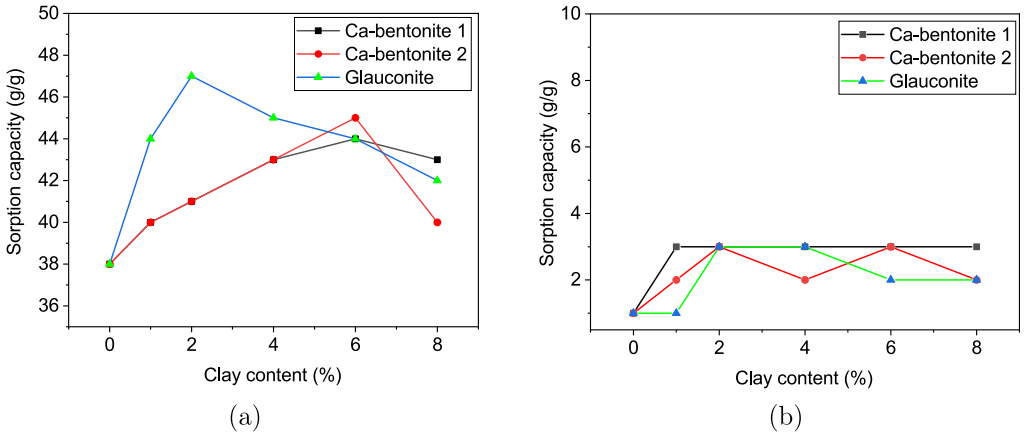

Figure 12. Sorption capacity of PVC/clay nanofiber mats: (a)—motor oil and (b)—water.

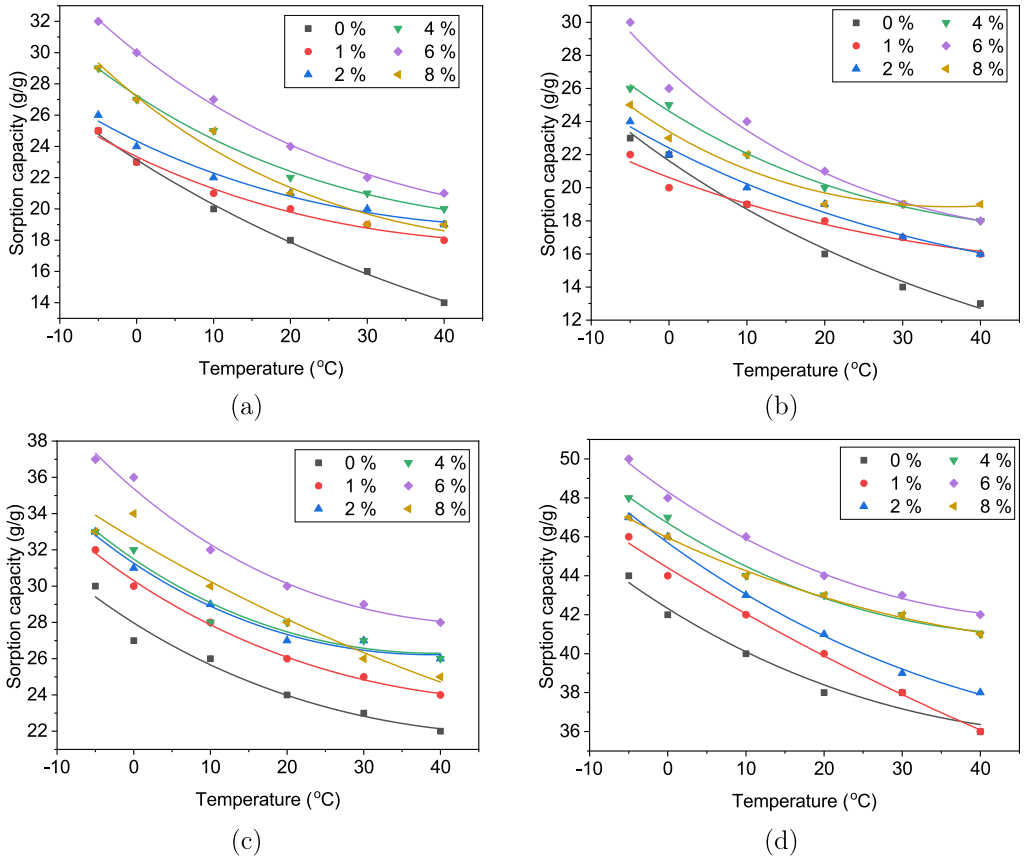

Figure 13. Effect of temperature on oil sorption capacity of PVC/Ca-bentonite 1 nanofiber mats: (a)—crude oil 1; (b)—crude oil 2; (c)—hydraulic oil; and (d)—motor oil.

influence of temperature on the sorption capacity of PVC/Ca-bentonite 2 and PVC/glauconite nanofiber mats). The study results show that the sorption capacity of nanofiber mats is inversely proportional to the temperature. The lower the temperature, the higher the sorption capacity of nanofiber mats. Even when the temperature increases to 40 °C, the nanofiber mats still have good sorption capacity. This shows that PVC/clay nanofiber mats have amazing potential as oil sorption materials for cold regions such as the arctic and/or hot regions such as the equator.

CONCLUSIONS

In this study, we successfully fabricated nanofibers from PVC and clays. Clay particles are present in nanofiber mats in two forms, covered with the polymer nanofiber or distributed in the empty space of the nanofiber mat. The presence of the clay particles in the PVC/clay nanofiber mats led to a change in its porosity, mechanical strength, and oil sorption capacity. When the clay particle is distributed in the voids of the nanofiber mats, they created a lift effect and gaps around the nanofibers. Therefore, the porosity of PVC/clay nanofiber mats is higher than that of pure PVC nanofiber mats. The tensile strength and Young's modulus of the PVC/clay nanofiber mats have changed

https://doi.org/10.1021/acsomega.1c02517
ACS Omega 2021, 6, 20512−20521

Table 3. Composition of the Substances of the PVC/Clay Solution

the concentration of solution wt %/v	mass of PVC (g)	mass of clay (Ca-bentonite 1, Ca-bentonite 2, and Glauconite) (g)	clay content, %	volume of THF (mL)	volume of DMF (mL)
15.2	3	0.03	1	10	10
15.3	3	0.06	2	10	10
15.6	3	0.12	4	10	10
15.9	3	0.18	6	10	10
16.2	3	0.24	8	10	10

depending on the content and diameter of the clay particles. For bentonite clay, the highest tensile strength value is found when the content of clay particles reaches 4%. For glauconite, the highest value of tensile strength is found when the content of clay particles reaches 1%. The change in porosity leads to an increased sorption capacity of the nanofiber mat. The sorption capacity of PVC/clay nanofiber mats at different temperatures has been studied, especially at negative temperatures. The results show that the PVC/clay nanofiber mat exhibits high sorption capacity to negative temperatures. Hence, they have the potential as a sorbent to remove oil in icy regions such as the arctic, where the other oil removal methods are inefficient or very expensive to remove.

MATERIALS AND METHODS

Materials. The PVC compound was obtained from Klöckner Pentaplast Rus Ltd. (Saint Petersburg, Russian Federation) with a molecular weight of M_w = 40,000 g/mol. *N*,*N*-Dimethylformamide (DMF) 99.9% was purchased from JSC EKOS-1 (Moscow, Russian Federation). Tetrahydrofuran (THF) 99.5% was purchased from Chemed Ltd. (Moscow, Russian Federation). All reagents were used as received without further purification. Bentonite clay 1 (Ca) was purchased from LLC "Baulux" (Almetyevsk, Russian Federation). Bentonite clay 2 (Ca) was purchased from LLC "Ataman" (Askan, Georgia). Glauconite was purchased from LLC "Glaukos" (Chelyabinsk, Russian Federation). Clay particles were dried at 100 °C for 24 h before being used.

Preparation of PVC/Clay Solution and Fabrication of Nanofibers. PVC was dissolved in a THF/DMF solvent mixture (1:1 by volume) to obtain a 15 % wt/v polymer solution.[40] The solution was stirred on a magnetic stirrer for 60 min at 50 °C to obtain a homogeneous solution. After that, clay was added into the solutions, and we continued stirring for another 60 min. The clay content and concentration of polymer in the solution are shown in Table 3. Then, we proceed to disperse the particles in an ultrasonic bath for 60 min at a temperature of 50 °C. The obtained solutions were used for the fabrication of nanofiber mats by the electrospinning method.

The electrospinning process is performed using the electrospinning system NANON-01A (Mecc Co., Ltd., Japan). The polymer solution is transferred into a 16 mm-diameter syringe with an 18 G metal needle (1.2 mm inner diameter). The conditions of the electrospinning process are as follows: voltage, 20 kV; feed rate, 0.5 mL/h; and the distance between the needle tip and collector, 15 cm. During electrospinning, a rotating drum collector was used with a rotation speed of 500 rpm. The nanofiber fabrication process was performed for 10 h. After that, a nanofiber mat was obtained on the collector surface. Nanofiber mats were dried at 50 °C for 24 h to remove the solvent before proceeding to the next experiments.

Determining Oil Sorption Capacity. The nanofiber mats were cut into samples with a size of 2 cm × 2 cm (average mass of 0.01 g) for the study of sorption capacity. After that, the nanofiber samples were immersed in glass beakers containing oil or water. After keeping the sample in the glass beakers for 10 min, the nanofiber mats are removed from the beaker and kept suspended for 2 min to drain drops. Then, the mass of the nanofiber mat was determined, after absorbing the oil, using an analytical balance with an accuracy of 0.0001 g.

Liquid cryothermostat FT-316-40 (LOIP Ltd., Russia) was used to maintain the temperature from −5 to +40 °C. First, the oils were thermally stabilized at a specific temperature. Once the oil reaches the required temperature, the PVC nanofibers were immersed in the oil. Similar experiments were performed for the determination of the sorption time.

The sorption capacity A (g/g) (oil/nanofiber) of nanofiber mats was calculated using the following equation

$$A = \frac{m_2 - m_1}{m_1} \quad (1)$$

where m_2 is the total mass of the nanofiber mats and absorbed oil, g, and m_1 is the mass of the nanofiber mat before sorption, g.

Table 4 shows the properties of the selected oils for testing with different viscosities.

Table 4. Oil Characteristics

parameter	crude oil 1	crude oil 2	hydraulic oil	motor oil
density, 25 °C, g/mL	0.828	0.810	0.865	0.875
viscosity, 25 °C, mPa·s	5.14	2.77	65.31	167.76
surface tension, mN/m	25.21	24.81	29.68	31.05

Measurements. The diameter distribution of clay was determined by the laser diffraction method using a particle diameter analyzer ANALYSETTE 22 MicroTec plus Fritsch (Idar-Oberstein, Germany).

The electrical conductivity of the polymer solution was determined on a WTW inoLab Cond 720 conductometer (Germany) with a WTW TetraCon 325 sensor. The measurement error was no more than 0.5%.

The nanofiber morphology was observed by SEM (Merlin, Carl Zeiss, Germany). The nanofiber diameters were analyzed using image processing software ImageJ (National Institutes of Health, USA).

XRD analysis was performed using an X-ray diffractometer DRON-8 with a BSV-29 sharp focus tube with a copper anode and a NaI scintillation detector. The scanning rate was 1°/min with the angle ranging from 5 to 50° (2θ).

Samples of nanofiber mats with dimensions of 2 cm × 2 cm were used to determine the density. The thickness of the sample was measured using the digital micrometer ABC (TechRim, Saint Petersburg, Russia) with an error of 0.1 μm.[41] The nanofiber mat is placed between two blank slides (Levenhuk G50) to minimize the force exerted on the nanofiber mats, and their thickness is measured with a micrometer screw. The

https://doi.org/10.1021/acsomega.1c02517
ACS Omega 2021, 6, 20512−20521

thickness of the nanofiber mat was obtained after subtracting the thickness of the blank slides. The mass of the sample was measured using an analytical balance with an error of 0.0001 g. The density (ρ) (g/cm^3) of the nanofiber mat is determined using the formula

$$\rho = \frac{m}{a \times b \times h} \quad (2)$$

where a is the length of the sample, cm; b is the width of the sample, cm; h is the thickness of the sample, cm; and m is the mass of the sample, g.

The porosity (P) of the nanofiber mats was calculated using the following equation

$$P = 1 - \frac{\rho}{\rho_0} \quad (3)$$

where ρ_0 is the bulk density of PVC 1.44 (g/cm^3).

The contact angle was measured using the lying drop method using a DSA100 drop shape analyzer (Kruss, Germany).

Mechanical properties were determined using the Instron 5943 testing machine with pneumatic grips (Instron, USA). The nanofiber mats were cut into samples with a size of 100 mm × 10 mm to study the tensile strength of the material. The test was carried out in accordance with ISO 527 with a tensile speed of 50 mm/min at room temperature. The test was carried out at a temperature of 23 ± 2 °C and a relative humidity of 35 ± 5%.

FTIR spectroscopy spectra of nanofiber mats were obtained using a Tensor 37 spectrometer (Bruker, Germany) using a MIRacle Pike Technologies ATR attachment equipped with a diamond-coated ZnSe crystal. The measurements were carried out with a spectral resolution of 2 cm^{-1} in the range 4000−600 cm^{-1} and averaging over 32 scans.

TGA was performed using a TG 209 F1 Libra (Netzsch, Germany) under a nitrogen atmosphere with a flow rate of 40 mL/min. The samples were studied in a range of temperatures that went from 25 to 900 °C with an increasing rate of 10 °C/min. Differential scanning calorimetry (DSC) studies were performed using a DSC 204 F1 Phoenix (Netzsch, Germany) under a nitrogen atmosphere with a flow rate of 20 mL/min. A single DSC measurement is carried out on increasing temperature. The samples were heated from −30 to 240 °C with an increasing rate of 10 °C/min.

■ ASSOCIATED CONTENT

Supporting Information

The Supporting Information is available free of charge at https://pubs.acs.org/doi/10.1021/acsomega.1c02517.

Thermal properties and oil sorption capacity of PVC/clay nanofiber mats; FTIR spectrum of PVC nanofiber mats; FTIR spectrum of clay particles; FTIR spectrum of PVC/clay nanofiber mats; TGA and DTA diagram of PVC nanofiber mats, clay particles, and PVC/clay nanofibers; TGA and DSC data of PVC/clay nanofibers; oil sorption capacity of PVC/clay nanofiber mats; and effect of temperature on the oil sorption capacity of PVC/clay nanofiber mats (PDF)

■ AUTHOR INFORMATION

Corresponding Author

Pham Le Quoc − *Institute BioEngineering, ITMO University, St. Petersburg 197101, Russia;* orcid.org/0000-0001-9134-8624; Phone: +79218782900; Email: quocphampro@gmail.com

Authors

Alexandra Y. Solovieva − *Institute BioEngineering, ITMO University, St. Petersburg 197101, Russia*

Mayya V. Uspenskaya − *Institute BioEngineering, ITMO University, St. Petersburg 197101, Russia*

Roman O. Olekhnovich − *Institute BioEngineering, ITMO University, St. Petersburg 197101, Russia*

Vera E. Sitnikova − *Institute BioEngineering, ITMO University, St. Petersburg 197101, Russia*

Inna E. Strelnikova − *Institute BioEngineering, ITMO University, St. Petersburg 197101, Russia*

Anisa M. Kunakova − *Gazprom Neft STC LLC, St. Petersburg 190000, Russia*

Complete contact information is available at: https://pubs.acs.org/10.1021/acsomega.1c02517

Notes

The authors declare no competing financial interest.

■ ACKNOWLEDGMENTS

This work was financially supported by ITMO University (project number 620170).

■ REFERENCES

(1) Ivshina, I. B.; Kuyukina, M. S.; Krivoruchko, A. V.; Elkin, A. A.; Makarov, S. O.; Cunningham, C. J.; Peshkur, T. A.; Atlas, R. M.; Philp, J. C. Oil spill problems and sustainable response strategies through new technologies. *Environ. Sci.: Processes Impacts* **2015**, *17*, 1201−1219.

(2) Asadpour, R.; Sapari, N.; Tuan, Z.; Jusoh, H.; Riahi, A.; Uka, O. Application of sorbent materials in oil spill management: a review. *Casp. J. Appl. Sci. Res.* **2013**, *2*, 46−58.

(3) Sarbatly, R.; Krishnaiah, D.; Kamin, Z. A review of polymer nanofibres by electrospinning and their application in oil−water separation for cleaning up marine oil spills. *Mar. Pollut. Bull.* **2016**, *106*, 8−16.

(4) Xu, Z.; Jiang, X.; Zhou, H.; Li, J. Preparation of magnetic hydrophobic polyvinyl alcohol (PVA)−cellulose nanofiber (CNF) aerogels as effective oil absorbents. *Cellulose* **2018**, *25*, 1217−1227.

(5) Xue, J.; Wu, T.; Dai, Y.; Xia, Y. Electrospinning and electrospun nanofibers: Methods, materials, and applications. *Chem. Rev.* **2019**, *119*, 5298−5415.

(6) Alghoraibi, I.; Alomari, S. Different Methods for Nanofiber Design and Fabrication. *Handbook of Nanofibers*; Springer International Publishing, 2019; Vol. *79−124*.

(7) Ramakrishna, S.; Fujihara, K.; Teo, W.-E.; Yong, T.; Ma, Z.; Ramaseshan, R. Electrospun nanofibers: Solving global issues. *Mater. Today* **2006**, *9*, 40−50.

(8) Pham, L. Q.; Uspenskaya, M. V.; Olekhnovich, R. O.; Olvera Bernal, R. A. A Review on Electrospun PVC Nanofibers: Fabrication, Properties, and Application. *Fibers* **2021**, *9*, 12.

(9) Gupta, R. K.; Bhattacharya, S. N. Polymer-clay nanocomposites: Current status and challenges. *Indian Chem. Eng.* **2008**, *50*, 242.

(10) Park, J. H.; Lee, H. W.; Chae, D. K.; Oh, W.; Yun, J. D.; Deng, Y.; Yeum, J. H. Electrospinning and characterization of poly(vinyl alcohol)/chitosan oligosaccharide/clay nanocomposite nanofibers in aqueous solutions. *Colloid Polym. Sci.* **2009**, *287*, 943−950.

(11) Shami, Z.; Sharifi-Sanjani, N. The role of Na-montmorillonite on thermal characteristics and morphology of electrospun PAN nanofibers. *Fibers Polym.* **2010**, *11*, 695−699.

(12) Hong, J. H.; Jeong, E. H.; Lee, H. S.; Baik, D. H.; Seo, S. W.; Youk, J. H. Electrospinning of polyurethane/organically modified montmorillonite nanocomposites. *J. Polym. Sci., Part B: Polym. Phys.* **2005**, *43*, 3171−3177.

(13) Uddin, F. Clays, nanoclays, and montmorillonite minerals. *Metall. Mater. Trans. A* **2008**, *39*, 2804−2814.
(14) Maxkamova, D.; Sodikova, S.; Usmonova, Z. *Bentonite Clay, Its Physico-Chemical Characteristics and Application in the National Economy*; Universum: Tekhnicheskiye Nauki, 2019; Vo. *6*.
(15) Li, Q.; Wei, Q.; Wu, N.; Cai, Y.; Gao, W. Structural characterization and dynamic water adsorption of electrospun polyamide6/montmorillonite nanofibers. *J. Appl. Polym. Sci.* **2008**, *107*, 3535−3540.
(16) Almuhamed, S.; Bonne, M.; Khenoussi, N.; Brendle, J.; Schacher, L.; Lebeau, B.; Adolphe, D. C. Electrospinning composite nanofibers of polyacrylonitrile/synthetic Na-montmorillonite. *J. Ind. Eng. Chem.* **2016**, *35*, 146−152.
(17) Park, J. H.; Karim, M. R.; Kim, I. K.; Cheong, I. W.; Kim, J. W.; Bae, D. G.; Cho, J. W.; Yeum, J. H. Electrospinning fabrication and characterization of poly(vinyl alcohol)/montmorillonite/silver hybrid nanofibers for antibacterial applications. *Colloid Polym. Sci.* **2010**, *288*, 115−121.
(18) Lee, Y. H.; Lee, J. H.; An, I.-G.; Kim, C.; Lee, D. S.; Lee, Y. K.; Nam, J.-D. Electrospun dual-porosity structure and biodegradation morphology of Montmorillonite reinforced PLLA nanocomposite scaffolds. *Biomaterials* **2005**, *26*, 3165−3172.
(19) Cai, J.; Lei, M.; Zhang, Q.; He, J.-R.; Chen, T.; Liu, S.; Fu, S.-H.; Li, T.-T.; Liu, G.; Fei, P. Electrospun composite nanofiber mats of Cellulose Organically modified montmorillonite for heavy metal ion removal: Design, characterization, evaluation of absorption performance. *Composites, Part A* **2017**, *92*, 10−16.
(20) Silva, D. B. R. d. S.; Júnior, L. P. C.; de Aguiar, M. F.; Alves, K. G. B.; Alves, K. G. Preparation and characterization of nanofibers of polyvinyl alcohol/polyaniline-montmorillonite clay. *J. Mol. Liq.* **2018**, *272*, 1070−1076.
(21) Yu, J.; Sun, L.; Ma, C.; Qiao, Y.; Yao, H. Thermal degradation of PVC: A review. *Waste Manage.* **2016**, *48*, 300−314.
(22) Shao, Z.; Jiang, J.; Wang, X.; Li, W.; Fang, L.; Zheng, G. Self-powered electrospun composite nanofiber membrane for highly efficient air filtration. *Nanomaterials* **2020**, *10*, 1706.
(23) Hezarjaribi, M.; Bakeri, G.; Sillanpää, M.; Chaichi, M. J.; Akbari, S. Novel adsorptive membrane through embedding thiol-functionalized hydrous manganese oxide into PVC electrospun nanofiber for dynamic removal of Cu(II) and Ni(II) ions from aqueous solution. *J. Water Process Eng.* **2020**, *37*, 101401.
(24) Zhu, H.; Qiu, S.; Jiang, W.; Wu, D.; Zhang, C. Evaluation of electrospun polyvinyl chloride/polystyrene fibers as sorbent materials for oil spill cleanup. *Environ. Sci. Technol.* **2011**, *45*, 4527−4531.
(25) Rivero, P. J.; Rosagaray, I.; Fuertes, J. P.; Palacio, J. F.; Rodríguez, R. J. Designing multifunctional protective PVC electrospun fibers with tunable properties. *Polymers* **2020**, *12*, 2086.
(26) Zhang, T.; Nazarov, R.; Pham, L. Q.; Soboleva, V.; Demchenko, P.; Uspenskaya, M.; Olekhnovich, R.; Khodzitsky, M. Polymer composites based on polyvinyl chloride nanofibers and polypropylene films for terahertz photonics. *Opt. Mater. Express* **2020**, *10*, 2456.
(27) Karim, M. R.; Lee, H. W.; Kim, R.; Ji, B. C.; Cho, J. W.; Son, T. W.; Oh, W.; Yeum, J. H. Preparation and characterization of electrospun pullulan/montmorillonite nanofiber mats in aqueous solution. *Carbohydr. Polym.* **2009**, *78*, 336−342.
(28) Uddin, F. Montmorillonite: An introduction to properties and utilization. *Curr. Top. Util. Clay Ind. Med. Appl.* **2018**, *1*, 3.
(29) Ji, H. M.; Lee, H. W.; Karim, M. R.; Cheong, I. W.; Bae, E. A.; Kim, T. H.; Islam, M. S.; Ji, B. C.; Yeum, J. H. Electrospinning and characterization of medium-molecular-weight poly(vinyl alcohol)/high-molecular-weight poly(vinyl alcohol)/montmorillonite nanofibers. *Colloid Polym. Sci.* **2009**, *287*, 751−758.
(30) Pham Le, Q.; Uspenskaya, M. V.; Olekhnovich, R. O.; Baranov, M. A. The Mechanical Properties of PVC Nanofiber Mats Obtained by Electrospinning. *Fibers* **2021**, *9*, 2.
(31) Unal, B.; Yalcinkaya, E. E.; Demirkol, D. O.; Timur, S. An electrospun nanofiber matrix based on organo-clay for biosensors: PVA/PAMAM-Montmorillonite. *Appl. Surf. Sci.* **2018**, *444*, 542−551.
(32) Ramesh, S.; Leen, K. H.; Kumutha, K.; Arof, A. K. FTIR studies of PVC/PMMA blend based polymer electrolytes. *Spectrochim. Acta, Part A* **2007**, *66*, 1237−1242.
(33) Sadak, E.; El-Komy, D.; Motawie, A. M.; Darwish, M. S.; Ahmed, S. M.; Mokhta, S. M. PVC - clay nanocomposites: Preparation, mechanical and thermal properties. *J. Sci. Res.* **2019**, *36*, 453−468.
(34) Abdel-Baset, T.; Elzayat, M.; Mahrous, S. Characterization and optical and dielectric properties of polyvinyl chloride/silica nanocomposites films. *Int. J. Polym. Sci.* **2016**, *2016*, 1707018.
(35) Hasan, M.; Lee, M. Enhancement of the thermo-mechanical properties and efficacy of mixing technique in the preparation of graphene/PVC nanocomposites compared to carbon nanotubes/PVC. *Prog. Nat. Sci.: Mater. Int.* **2014**, *24*, 579−587.
(36) Kaushik, A.; Ahuja, D.; Salwani, V. Synthesis and characterization of organically modified clay/castor oil based chain extended polyurethane nanocomposites. *Composites, Part A* **2011**, *42*, 1534−1541.
(37) TIP 08: Use of sorbent materials in oil spill response, 2014. https://www.itopf.org/knowledge-resources/documents-guides/document/tip-08-use-of-sorbent-materials-in-oil-spill-response (accessed June 16, 2021).
(38) Le, Q. P.; Olekhnovich, R. O.; Uspenskaya, M. V.; Vu, T. H. N. Study on polyvinyl chloride nanofibers ability for oil spill elimination. *Iran. Polym. J.* **2021**, *30*, 473−483.
(39) Pigłowski, J. Temperature dependence of surface tension of poly(vinyl chloride). *Angew. Makromol. Chem.* **1985**, *136*, 193−194.
(40) Pham, L. Q.; Uspenskaya, M. V. Morphalogy PVC nanofiber, produced by electrospinning method. *19th International Multidisciplinary Scientific GeoConference SGEM 2019*, 2019; Vol. *19*, pp 289−295.
(41) Aussawasathien, D.; Teerawattananon, C.; Vongachariya, A. Separation of micron to sub-micron particles from water: electrospun nylon-6 nanofibrous membranes as pre-filters. *J. Membr. Sci.* **2008**, *315*, 11−19.

https://doi.org/10.1021/acsomega.1c02517
ACS Omega 2021, 6, 20512−20521